Supplementary materials

## Supplementary methods

*Near-infrared fluorescence imaging*

Mice received a single intravenous injection with DiR (0.5 mg/kg) labeled mTORi-NB (5 mg/kg) or S6K1i-NB (5 mg/kg). Liver, spleen, lung, kidneys, heart and muscle tissue were collected for NIRF imaging. Fluorescent images were acquired using an IVIS 200 system (Xenogen), with a 2 second exposure time, using a 745 nm excitation filter and an 820 nm emission filter. Regions of interest (ROIs) were drawn on each tissue with software provided by the vendor, after which quantitative analyses were performed using the average radiant efficiency within these ROIs.

*Preparation of single-cell suspensions for flow cytometry*

Blood was collected by cardiac puncture and mice were subsequently perfused with 20 mL cold PBS. Spleen and femurs were harvested. The aorta, from aortic root to the iliac bifurcation, was gently cleaned of fat and collected. The aorta was digested using an enzymatic digestion solution containing liberase TH (4 U/mL) (Roche), deoxyribonuclease (DNase) I (40 U/mL) (Sigma-Aldrich), and hyaluronidase (60 U/mL) (Sigma-Aldrich) in PBS at 37 °C for 60 minutes. Cells were filtered through a 70 μm cell strainer and washed with serum-containing PBS. Blood was incubated with lysis buffer (BD Biosciences) for 4 minutes and washed with serum-containing PBS. Spleens were mashed, filtered through a 70 μm cell strainer, incubated with lysis buffer for 4 minutes and washed with serum-containing PBS. Bone marrow was flushed out of the femur with PBS, filtered through a 70 μm cell strainer, incubated with lysis buffer for 30 seconds and washed with serum-containing PBS.

*Flow cytometry*

Single-cell suspensions from the aorta, blood, spleen and bone marrow were stained with the following monoclonal antibodies: anti-CD11b (clone M1/70, BioLegend), anti-F4/80

(clone BM8, BioLegend); anti-CD11c (clone N418, BioLegend), anti-CD45 (clone 30-F11, BioLegend), anti-Ly6C (clone AL-21, BD Biosciences), and a lineage antibody cocktail (Lin) containing anti-CD90.2 (clone 53-2.1, eBioScience), anti-Ter119 (clone TER119, eBioScience), anti-NK1.1 (clone PK136, eBioScience), anti-CD49b (clone DX5, eBioScience), anti-CD45R (clone RA3-6B2, eBioScience) and anti-Ly6G (clone 1A8, BioLegend). Hematopoietic stem and progenitor cells were identified by staining bone marrow cells with: anti-CD117 (c-Kit, clone 2B8, BioLegend), anti-Sca1 (clone E13-161.7, BioLegend), anti-CD48 (clone HM48-1, BioLegend), anti-CD150 (clone TC15-12F12.2, BioLegend) and a commercially available lineage antibody cocktail (BD Biosciences) containing anti-CD3e (clone 500A2), anti-CD11b (clone M1/70), anti-CD45R/B220 (clone RA3-6B2), anti-Ly-76 (clone TER-119), anti Ly6C and anti-Ly6G (both clone RB6-8C5).The contribution of newly made cells to different populations was determined by in vivo labeling with 5-Bromo-2'-deoxy-uridine (BrdU, BD Biosciences). Mice were injected with 1 mg BrdU 24 hours before euthanasia. BrdU flow kits were used according to the manufacturer's protocol. Data were acquired on a BD LSRII and a BD LSRFortessa flow cytometer (BD Biosciences). DiO signal was detected in the FITC channel. Counting beads were added to calculate absolute cell numbers. Data were analyzed using FlowJo v10.0.7 (Tree Star).

*Fluorescence molecular tomography with CT*

After nanobiologic treatment, mice were injected with 5 nanomoles of pan-cathepsin protease sensor (ProSense 680, PerkinElmer, Cat no. NEV10003). Twenty-four hours later, animals were placed in a custom built cartridge and sedated during imaging with continuous isoflurane administration as described previously (*10*). Animals were first scanned using a high-resolution CT scanner (Inveon PET-CT, Siemens), with a continuous infusion of CT-contrast agent (isovue-370, Bracco Diagnostics) at a rate of 55 μL/min through a tail vein catheter. Animals were subsequently scanned using an FMT scanner (PerkinElmer) in the same cartridge. The CT X-ray source with an exposure time of 425 milliseconds over 360 projections, was operated at 80 kVp and 500 μA. CT images were reconstructed using a modified Feldkamp cone beam reconstruction algorithm

(COBRA, Exxim Inc) Contrast-enhanced high-resolution CT images were used to localize the aortic root, which was used to guide the placement of the volume of interest for the quantitative FMT protease activity map. Image fusion relied on fiducial markers built into the imaging cartridge. Image fusion and analysis were performed using OsiriX v.6.5.2 (The Osirix Foundation, Geneva).

*Laser capture microdissection*

Laser capture microdissection was performed on 24 aortic root sections (6 μm). Frozen sections were dehydrated in graded ethanol solutions (70% twice, 95% twice, 100% once), washed with diethylpyrocarbonate (DEPC)-treated water, stained with Mayer's H&E and cleared in xylene. For every 8 sections, 1 section was used for CD68 staining (Abd Serotec, 1:250 dilution, MCA1957), which was used to guide the laser capture microdissection. CD68-rich areas within the plaques were identified and collected using an ArcturusXT LCM System.

*RNA sequencing analysis of murine plaque macrophages*

For RNA sequencing analysis of $CD68^+$ cells isolated from the murine aortic plaque, the pair-ended sequencing reads were aligned to human genome hg19 using TopHat aligner (bowtie2) *(61)*. Next, HTSeq *(62)* was used to quantify the gene expression at the gene level based on GENCODE gene model release 22 *(63)*. Gene expression raw read counts were normalized as counts per million using trimmed mean of M-values normalization method to adjust for sequencing library size difference among samples. DEGs between drug treatments and control were identified using the Bioconductor package limma *(64)*. In order to correct the multiple testing problem, limma was used to calculate *t*-statistics by permuting sample labels. This procedure was repeated 1,000 times to obtain a null *t*-statistic distribution for estimating the false discovery rate (FDR) values of all genes. The DEGs of cells isolated from the aortic plaques were identified using a cut-off at an FDR of less than 0.05. A weighted gene co-expression network analysis (WGCNA) was constructed to identify groups of genes (modules) involved in various activated pathways following a previous described algorithm *(65)*. In short, Pearson correlations were computed between each pair of genes yielding a similarity (correlation) matrix (sij).

Subsequently a power function (aij = Power (sij, β) ≡ | sij | β), was used to transform the similarity matrix into an adjacency matrix A [aij], where aij is the strength of a connection between two nodes (genes) i and j in each module. For all genes the connectivity (*k*) was determined by taking the sum of their connection strengths with all other genes in the network. The parameter was chosen by using the scale-free topology criterion, such that the resulting network connectivity distribution approximated scale-free topology. The adjacency matrix was then used to define a measure of node dissimilarity, based on the TOM. The module subnetworks were visualized using MEGENA and cytoscape *(66, 67)*. To identify gene modules, we performed hierarchical clustering on the TOM. Modules were analyzed with the online annotation tool from the protein annotation through evolutionary relationship (PANTHER) Classification System.

*siRNA nanotherapeutic formulation and analysis*

*Psap* siRNA (sequence: 5'- rArUrA rArGrU rUrUrU rCrUrG rArGrC rUrGrA rUrUrG rUrCA A -3' and 5'- rUrUrG rArCrA rArUrC rArGrC rUrCrA rGrArA rArArC rUrUrA rUrUrC -3') was purchased from Integrated DNA Technologies. SiRNA (0.176 mg, 10 nmol) was dissolved in nuclease free duplex buffer (7.65 µL), Milli-Q water (3.156 mL), and NaOAc buffer (1.056 mL, 25 mM, pH 4.0). Separately, an ethanol solution (2 mL) containing MC3 (DLin-MC3-DMA, 5.84 mg, 9.10 µmol), DSPC (1.59 mg, 2.01 µmol), cholesterol (3.30 mg, 8.54 µmol), and PEG-DSG (1.31 mg, 0.50 µmol) was created. The siRNA and lipid solutions were microfluidically mixed using BS-2000 microfluidic pumps (Braintree) and a T-junction (made in-house from poly ether ether ketone (PEEK) HPLC tubing, details are available on request) (injecting 3.00 mL of siRNA solution at 15.0 mL/min and 1.00 mL lipid solution at 5.01 mL/min). Directly afterwards, the solution was dialyzed (10.000 MWCO) against PBS (400 mL) at 4 °C for 2 days; PBS was refreshed twice during this period. The crude nanotherapeutics were filtered using a 0.2 µm PES syringe filter and concentrated using centrifugal filtration (Vivaspin, 100 kDa MWCO, 4000 rpm, 4 °C). The obtained nanoparticles had a mean size of approximately 32 nm, as determined by dynamic light scattering.

To determine siRNA recovery and entrapment, PBS or nanotherapeutics (50 µL) were mixed with Tris-EDTA (TE) buffer (50 µL), in a 96 well plate. Separately, PBS or

nanotherapeutics were mixed with TE buffer containing 2% Triton X-100 (50 µL). Lastly, an identical NaOAc buffered siRNA solution as used to formulate the nanotherapeutics was diluted with PBS to obtain siRNA calibrants (0, 8, 16, 32, 40 µg/mL, 50 µL each) which were subsequently mixed with TE buffer containing 2% Triton X-100 (50 µL). The 96 well plate was incubated at 37 °C for 10 minutes. QuantIT RiboGreen was diluted 100x with TE buffer and 100 µL added to each well. Fluorescence intensity was measured directly after (excitation/emission = 490/530 nm). The fluorescent intensities of the respective PBS samples were regarded as background and subtracted from all other samples.

The samples treated with TE buffer will only show the amount of siRNA present in the sample that is not incorporated in the nanotherapeutics. In contrast, the samples treated with TE buffer containing 2% Triton X-100 will show the total amount of siRNA in the sample.

*Recovery* = 100% * amount of siRNA found in the sample / amount of siRNA used to formulate the nanotherapeutics.

*Entrapment* = 100% * fraction of siRNA in the sample that is inside the nanotherapeutics.

*Metabolic extracellular flux analysis*

Murine BMDMs were plated at 2.5-5.0 x$10^4$ cells/well in an XF-96-cell culture plate (Seahorse Bioscience) and left to adhere. BMDMs were incubated with mTORi (20µM), S6K1i (20µM) or DMSO (control) for 16 hours. In a separate assay BMDMs were incubated with Psap siRNA-LNPs (0.5 µg/mL), Ctrl SiRNA-LNPs (0.5 µg/mL) or PBS for 24 hours. The extracellular acidification rate (ECAR) and oxygen consumption rate (OCR) in response to glucose (10 mM), oligomycin (OM, 1.5 µM), carbonyl cyanide 4-(trifluoromethoxy)phenylhydrazone (FCCP, 1.5 µM), and rotenone (ROT, 1.25 µM) + antimycin A (AA, 2.5 µM) injections were measured using a Seahorse XFe96 Analyzer (Agilent). Upon completion, DNA content was measured with CyQuant to compensate for differences in cell numbers. The maximal glycolytic capacity was determined by the difference in ECAR between baseline and FCCP stimulated cells. The maximal respiratory capacity was calculated using the difference in OCR between FCCP and Rot/AA stimulated cells.

*Human PBMC and monocyte isolation*

PBMC isolation was performed by dilution of blood in pyrogen-free PBS and differential density centrifugation over Ficoll-Paque. Cells were washed three times in PBS. Percoll isolation of monocytes was performed as previously described. Briefly, 150-200x$10^6$ PBMCs were layered on top of a hyper-osmotic Percoll solution (48.5% Percoll, 41.5% sterile $H_2O$, 0.16M filter sterilized NaCl) and centrifuged for 15 minutes at 580 g. The interphase layer was isolated and cells were washed once with cold PBS. Cells were resuspended in RPMI culture medium supplemented with 50 µg/ml gentamicin, 2 mM glutamax, and 1 mM pyruvate and counted using a Beckman Coulter counter. An extra purification step was added by adhering Percoll isolated monocytes to polystyrene flat bottom plates (Corning, NY, USA) for 1 hour at 37 °C; subsequently a washing step with warm PBS was performed to yield maximal purity. This increases purity to only 3% T cell contamination as previously described *(68)*.

*Preparation of oxidized LDL*

LDL was isolated using KBr-density gradient ultracentrifugation from serum from healthy volunteers. Plasma density was adjusted to ρ=1.100 g/mL with KBr. The samples were centrifuged for 22h at 32.000 rpm in a SW41 Ti rotor. Oxidized LDL was prepared by incubation of LDL with 20 µmol $CuSO_4$/L for 15 hours at 37 °C in a shaking water bath as described previously *(69)*.

*Human monocyte in vitro experiments*

For oxLDL and prosaposin priming experiments, 100,000 cells were added to flat-bottom 96-well plates. After washing with warm PBS, monocytes were incubated either with culture medium only as a negative control, 10 µg/mL oxLDL or 200 ng/mL prosaposin (Abcam, ab203534) for 24 hours (in 10% pooled human serum). Cells were washed once with 200 µl of warm PBS and incubated for 5 days in culture medium with 10% pooled human serum, and medium was refreshed once. Cells were re-stimulated with LPS (10 ng/mL) for 4 hours before applying them to single-cell RNA sequencing in the well-based platform SORT-seq *(57)*. For cytokine measurements, cells were stimulated with LPS

during 24 hours. Subsequently, supernatants were collected and stored at -20 °C until cytokine measurement. In some experiments, cells were pre-incubated (before oxLDL stimulation) for 1 hour with nanobiologics (10 μM mTORi-NB, 0.1 μM S6K1i-NB or corresponding quantities of unloaded NB). After 24 hours, both oxLDL and nanobiologics were washed away and cells were let to rest for 5 days as described above.

*Cytokine measurements*

Cytokine production was determined in supernatants using commercial ELISA kits (R&D systems) for human TNFα and IL-6 following the instructions of the manufacturer.

*Single-cell RNA sequencing analysis of human monocytes*

For human monocyte single-cell RNA sequencing analysis, the sequencing data was aligned to human hg19 transcriptome. Subsequently *Seurat* (v3.1) *(70)* was used for downstream analyses. Quality controls were applied to remove low quality cells, which were defined as cells in which fewer than 100 or higher than 7000 unique genes were detected, or cells with higher than 25% mitochondrial counts. Based on a hierarchical clustering of the single-cell RNA profiles we found a subgroup of macrophages with high expression of chemokine markers (*CXCL9, CXCL10, CXCL11*). By using Wilcoxon rank sum test, differential expression analysis of *PSAP* was performed.

*Human plaque processing for bulk RNA-seq*

To assess the global expression profile, plaque segments (n=700) were thawed, cut into pieces, and further homogenized using ceramic beads and tissue homogenizer (Precellys, Bertin instruments, Montigny-le-Bretonneux, France), in the presence of TriPure (Sigma Aldrich). From this homogenized mix RNA was isolated as per TriPure manufacturer's protocol. Then, RNA in the aqueous phase was precipitated with isopropanol, washed with 75% ethanol, and subsequently stored in 75% ethanol for later use or used immediately after an additional washing step with 75% ethanol.

*Library preparation for bulk RNA-seq*

Library preparation was performed, adapting the CEL-Seq2 protocol for library preparation *(71, 72)*, as described before *(73)*. After removing ethanol, and air-drying the pellet, primer mix containing 5ng primer per reaction was added, initiating primer annealing at 65 °C for 5min. Subsequent reverse-transcription RT reaction; first strand reaction for 1h at 42 °C, heat inactivated for 10m at 70°C, second strand reaction for 2 hours at 16 °C, and then put on ice until proceeding to sample pooling. This initial RT reaction used the following primer design: an anchored polyT, a unique 6bp barcode, a unique molecular identifier (UMI) of 6bp, the 5' Illumina adapter and a T7 promoter, as described *(73)*. Each sample now contained its own unique barcode making it possible to pool together cDNA samples at 7 samples per pool. Complementary DNA (cDNA) was cleaned using AMPure XP beads (Beckman Coulter), washed with 80% ethanol, and resuspended in water before proceeding to the in vitro transcription (IVT) reaction (AM1334; Thermo-Fisher) incubated at 37 °C for 13 hours. Next, Exo-SAP (Affymetrix, Thermo-Fisher) was used to remove primers, upon which amplified RNA (aRNA) was fragmented, cleaned with RNAClean XP (Beckman-Coulter), washed with 70% ethanol, air-dried, and resuspended in water. After removing the beads by using a magnetic stand, RNA yield and quality in the suspension were checked by Bioanalyzer (Agilent).
cDNA libraries were then built by performing an RT reaction using SuperScript II reverse transcriptase (Invitrogen/Thermo-Fisher) according to the manufacturer's protocol, including randomhexRT primer as random primer. Next, PCR amplification was done with Phusion High-Fidelity PCR Master Mix with HF buffer (NEB, MA, USA) and a unique indexed RNA PCR primer (Illumina) per reaction, for a total of 11-15 cycles, depending on aRNA concentration, with 30 seconds elongation time. PCR products were cleaned twice with AMPure XP beads (Beckman Coulter). Library cDNA yield and quality were checked by Qubit fluorometric quantification (Thermo-Fisher) and Bioanalyzer (Agilent), respectively. Libraries were sequenced on the Illumina Nextseq500 platform; paired end, 2 x 75bp.

*Bulk RNA sequencing analysis Athero-Express samples*

For bulk RNA-seq analysis of human atherosclerotic plaque samples, fastq files were de-barcoded, and split into forward and reverse reads. These were mapped making use of

Burrows-Wheel aligner (BWA) *(74)* version 0.7.17-r1188, calling 'bwa aln' with settings -B 6 -q 0 -n 0.00 -k 2 -l 200 -t 6 for R1 and -B 0 -q 0 -n 0.04 -k 2 -l 200 -t 6 for R2, 'bwa sampe' with settings -n 100 -N 100, and a cDNA reference (assembly hg19, Ensembl release 84). Read counts and UMI counts were derived from SAM files using custom perl code, and then, using R version 3.6.3 and Rstudio IDE version 1.2.1335 for further analyses, gathered into count matrices. Genes were annotated with Ensembl ID's, and basic quality control was performed. Samples with low gene numbers (<10,000 genes), and read numbers (<18,000 reads) were filtered out. Resulting number of samples: 641, with 60,674 genes (Ensembl ID's), and median of 178,626 reads per sample.
Counts, metadata and clinical data were combined into a SummarizedExperiment object. Counts were pre-filtered, normalized and transformed making use of the variance stabilization transformation function (vst) *(75)* in DESeq2, resulting in transformed data of n=620 on a log2-scale, normalized for library size. These were used to compare PSAP expression to the expression of a random sample of 1000 genes, and to assess correlations between genes, to construct correlation heatmaps and correlation scatter plots. Correlation estimates and p-values were calculated using Spearman's rank correlation. Heatmaps were drawn using Pheatmap from the Pheatmap package, applying hierarchical clustering based on correlation estimates, applying standard settings: complete linkage and Euclidean distance.

*Human plaque processing for single-cell RNA-seq*

Plaque segments (n=18) were washed in RPMI and cut up into small pieces (~1 $mm^3$). Nest, tissue was digested using a mix of RPMI 1640, 2.5 mg/mL Collagenase IV (Thermo Fisher Scientific), 0.25 mg/mL DNAse I (Sigma), 2.5 mg/mL Human Albumin Fraction V (MP Biomedicals) and 1 mM Flavopiridol (Selleckchem), incubating at 37 °C for 30 minutes. The resulting cell suspension was filtered using a 70 µm cell strainer and washed with RPMI 1640. Cells were kept in RPMI 1640 containing 1% Fetal Calf Serum until subsequent staining for cell sorting by flow cytometry.

*Cell sorting by flow cytometry for single-cell RNA-seq*

Cells were washed and then stained with Calcein AM and Hoechst (Thermo Fisher Scientific) in PBS supplemented with 5% Fetal Bovine Serum (FBS) and 0.2% ethylenediaminetetraacetic acid (EDTA) for 30 minutes at 37 °C. Subsequently, cells were washed, filtered (70 µm FlowMi cell strainer; SP Scienceware), upon which Calcein AM and Hoechst double-positive viable cells were sorted using a MoFlo Astrios EQ cell sorter (Beckman Coulter).

*Single cell RNA-sequencing*

Viable cells were single-cell sorted into these 384 wells plates containing 50 nL mineral oil, CELseq2-primers, spike-ins and dinucleotide triphosphates (dNTPs). Afterwards, plates were immediately sealed and frozen at -80 °C until further processing. First, cDNA was constructed using the SORT-seq protocol *(57)*. In short, cells were lysed for 5 minutes at 65 °C upon which reverse transcription and second strand mixes were making use of a Nanodrop II liquid handling platform (GC biotech) Then, cells were pooled into one library. The aqueous phase was separated from the oil phase, followed by in vitro transcription (IVT). The CEL-Seq2 protocol *(71, 72)* was used to construct a library, with the following primers design: a 24 bp polyT stretch, a 64bp random UMI, a cell-specific 8bp barcode, the 5′ Illumina TruSeq small RNA kit adapter and a T7 promoter. For sequencing, TruSeq small RNA primers (Illumina) were added to the libraries and sequenced paired end at 75 bp read length using an Illumina NextSeq 500.

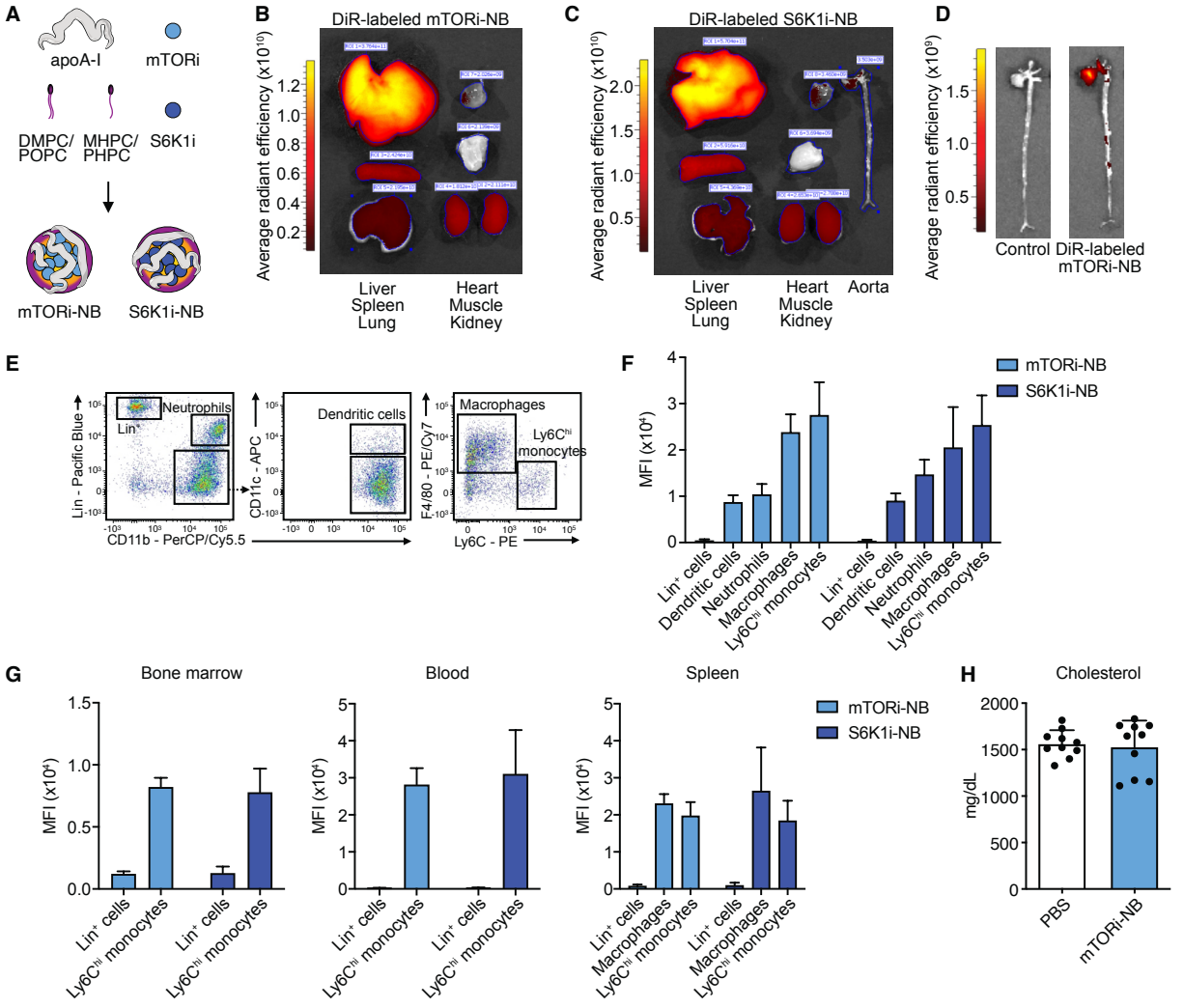


**Fig. S1. Characteristics of mTORi-NB and S6K1i-NB.** Related to Fig. 1. (**A**) Schematic overview of the different components of mTORi-NB and S6K1i-NB. mTORi-NB was constructed by combining human apoA-I, the phospholipids 1,2-dimyristoyl-sn-glycero-3-phosphocholine (DMPC) and 1-myristoyl-2-hydroxy-sn-glycero-phosphocholine (MHPC) and the mTOR inhibitor rapamycin. S6K1i-NB consisted of apoA-I, the phospholipids 1-palmitoyl-2-oleoyl-sn-glycero-3-phosphocholine (POPC) and 1-palmitoyl-2-hydroxy-sn-glycero-3-phosphocholine (PHPC), and the S6K1 inhibitor PF-4708671. (**B,C**) IVIS imaging of organs of *Apoe*$^{-/-}$ mice, injected with DiR-labeled mTORi-NB (**B**) or DiR-labeled S6K1i-NB (**C**). Organs were harvested 24 hours after injection. (**D**) IVIS imaging of the aorta of DiR-labeled mTORi-NB injected *Apoe*$^{-/-}$ mice. (**E-G**) *Apoe*$^{-/-}$ mice were injected with DiO-labeled mTORi-NB or DiO-labeled S6K1i-NB and euthanized 24 hours later. (**E**) Flow cytometry gating strategy of CD45$^{+}$ cells in the whole aorta and (**F**) quantification of DiO signal in each cell type. (*n* = 2-4 mice/group). (**G**) Quantification of DiO signal in leukocyte populations in the spleen, bone marrow and blood. (*n* = 4 mice/group). (**H**) *Apoe*$^{-/-}$ mice were fed a Western diet for 12 weeks, followed by 1 week of treatment, while continuing the diet. Treatment consisted of 4 intravenous injections of control (PBS) or mTORi-NB. Graph shows blood cholesterol of *Apoe*$^{-/-}$ mice after mTORi-NB treatment as compared to PBS. Experiments were performed once. Data are presented as mean ± SD, a non-parametric Mann-Whitney U test was used in H. DiR, $DiIC_{18}(7)$; DiO, $DiOC_{18}(3)$

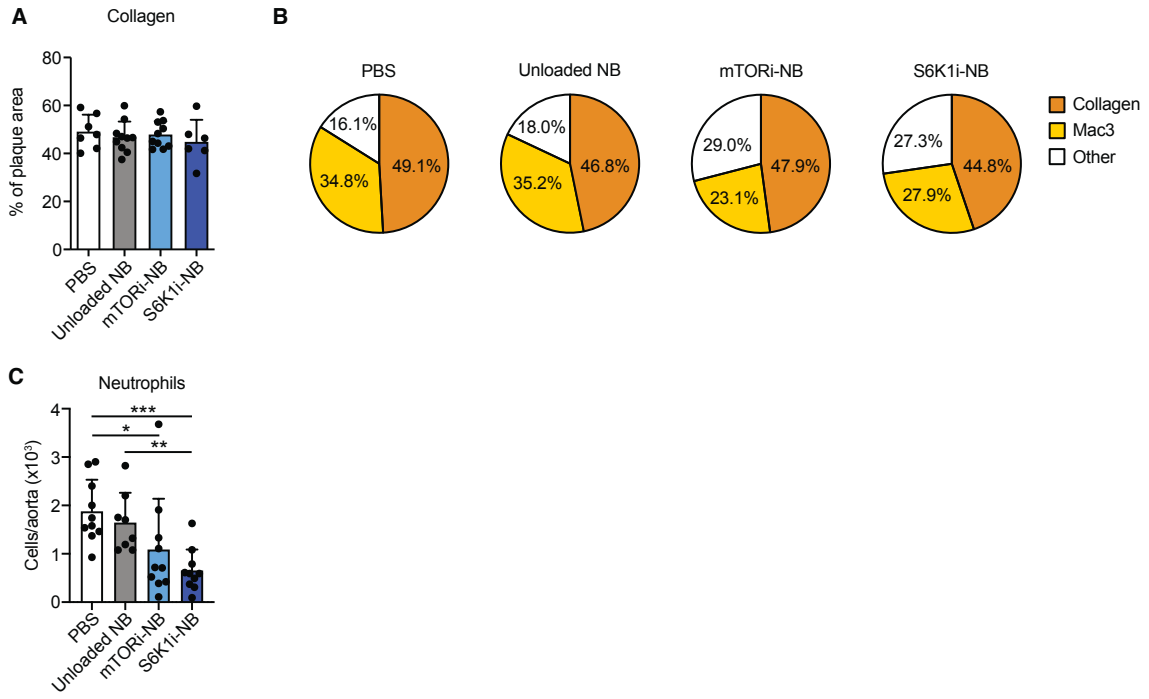


**Fig. S2. Myeloid cell-specific mTOR inhibition reduces atherosclerotic plaque inflammation.** Related to Fig. 1. *Apoe*$^{-/-}$ mice were fed a Western diet for 12 weeks, followed by 1 week of treatment, while continuing the diet. Treatment consisted of 4 intravenous injections of PBS, unloaded nanobiologics, mTORi-NB or S6K1i-NB. (**A**) Aortic plaque collagen content expressed as percentage of plaque area, assessed by Sirius Red staining ($n$ = 6-10 mice/group). (**B**) Relative contributions of collagen and Mac3$^{+}$ areas to the aortic plaque. (**C**) Flow cytometry analysis of neutrophils (CD11b$^{+}$Lin$^{+}$) in the aorta ($n$ = 8-10 mice/group). Experiments were performed once. Bar graphs are presented as mean ± SD, non-parametric Mann-Whitney U tests were used in A and C. *$P$ < 0.05, **$P$ < 0.01, ***$P$ < 0.001.

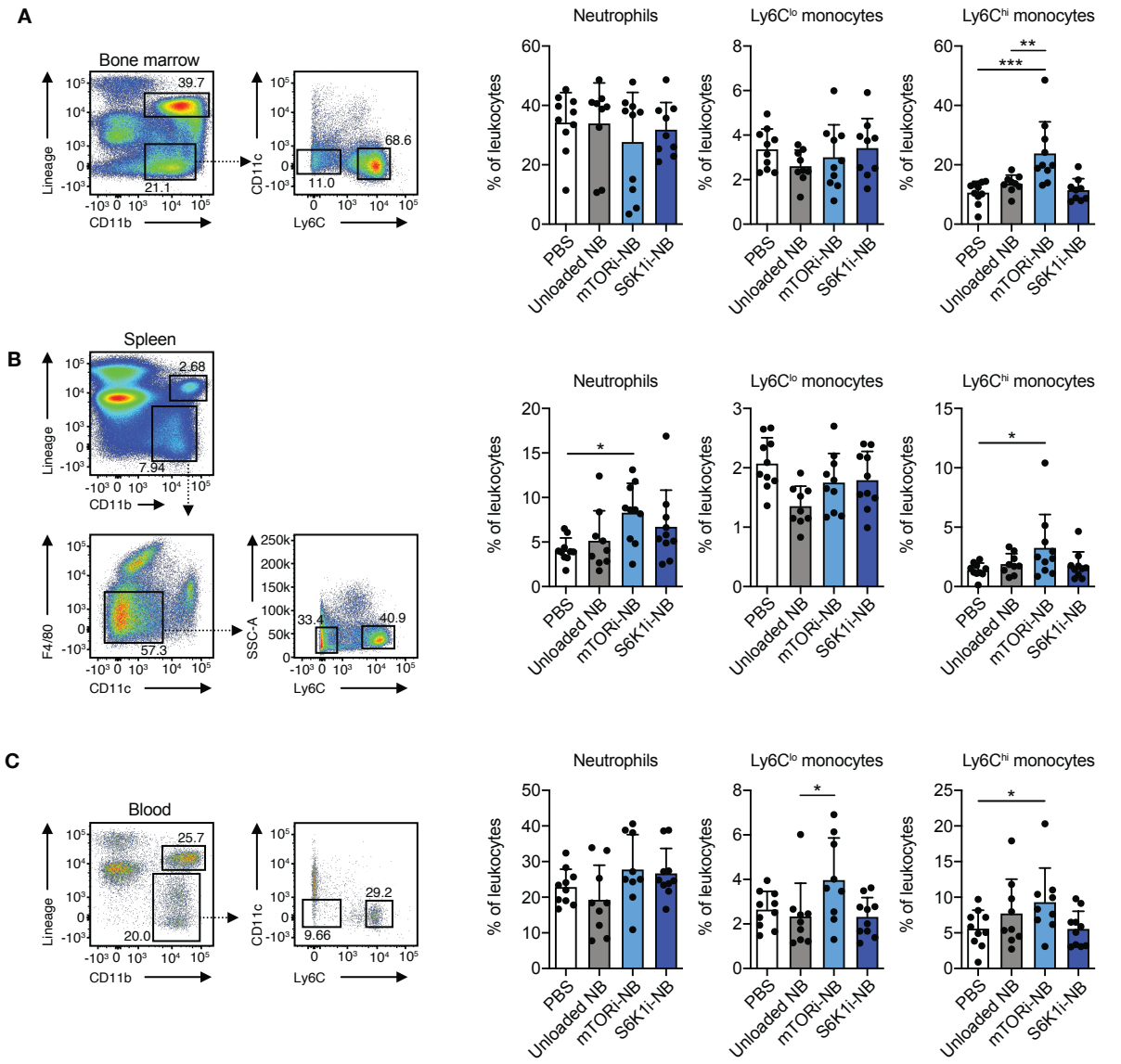


**Fig. S3. Systemic effects of mTORi-NB and S6K1i-NB treatment.** Related to Fig. 1. *Apoe*$^{-/-}$ mice were fed a Western diet for 12 weeks, followed by 1 week of treatment, while continuing the diet. Treatment consisted of 4 intravenous injections of PBS, unloaded nanobiologics, mTORi-NB or S6K1i-NB ($n$ = 9-10 mice/group for all panels). (**A**) Gating strategy and quantification of neutrophils (CD11b$^+$Lin$^+$), Ly6C$^{lo}$ (CD11b$^+$Lin$^-$CD11c$^-$Ly6C$^{lo}$) and Ly6C$^{hi}$ (CD11b$^+$Lin$^-$CD11c$^-$Ly6C$^{hi}$) monocytes in the bone marrow. (**B**) Gating strategy and quantification of neutrophils (CD11b$^+$Lin$^+$), Ly6C$^{lo}$ (CD11b$^+$Lin$^-$CD11c$^-$F4/80$^-$Ly6C$^{lo}$) and Ly6C$^{hi}$ (CD11b$^+$Lin$^-$CD11c$^-$F4/80$^-$Ly6C$^{hi}$) monocytes in the spleen. (**C**) Gating strategy and quantification of neutrophils (CD11b$^+$Lin$^+$), Ly6C$^{lo}$ (CD11b$^+$Lin$^-$CD11c$^-$Ly6C$^{lo}$) and Ly6C$^{hi}$ (CD11b$^+$Lin$^-$CD11c$^-$Ly6C$^{hi}$) monocytes in peripheral blood. Experiments were performed once. Bar graphs are presented as mean ± SD, non-parametric Mann-Whitney U tests were used. *$P$ < 0.05, **$P$ < 0.01, ***$P$ < 0.001.

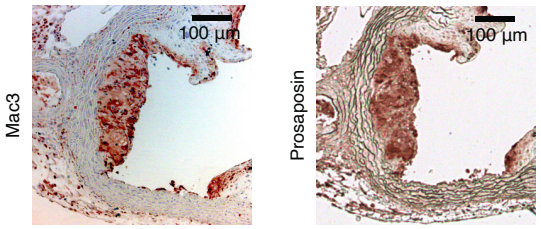


**Fig. S4. Prosaposin colocalizes with macrophages in murine plaques.** Related to Fig. 2. Representative histologic images of murine atherosclerotic plaques. Staining for macrophages (Mac3) and prosaposin.

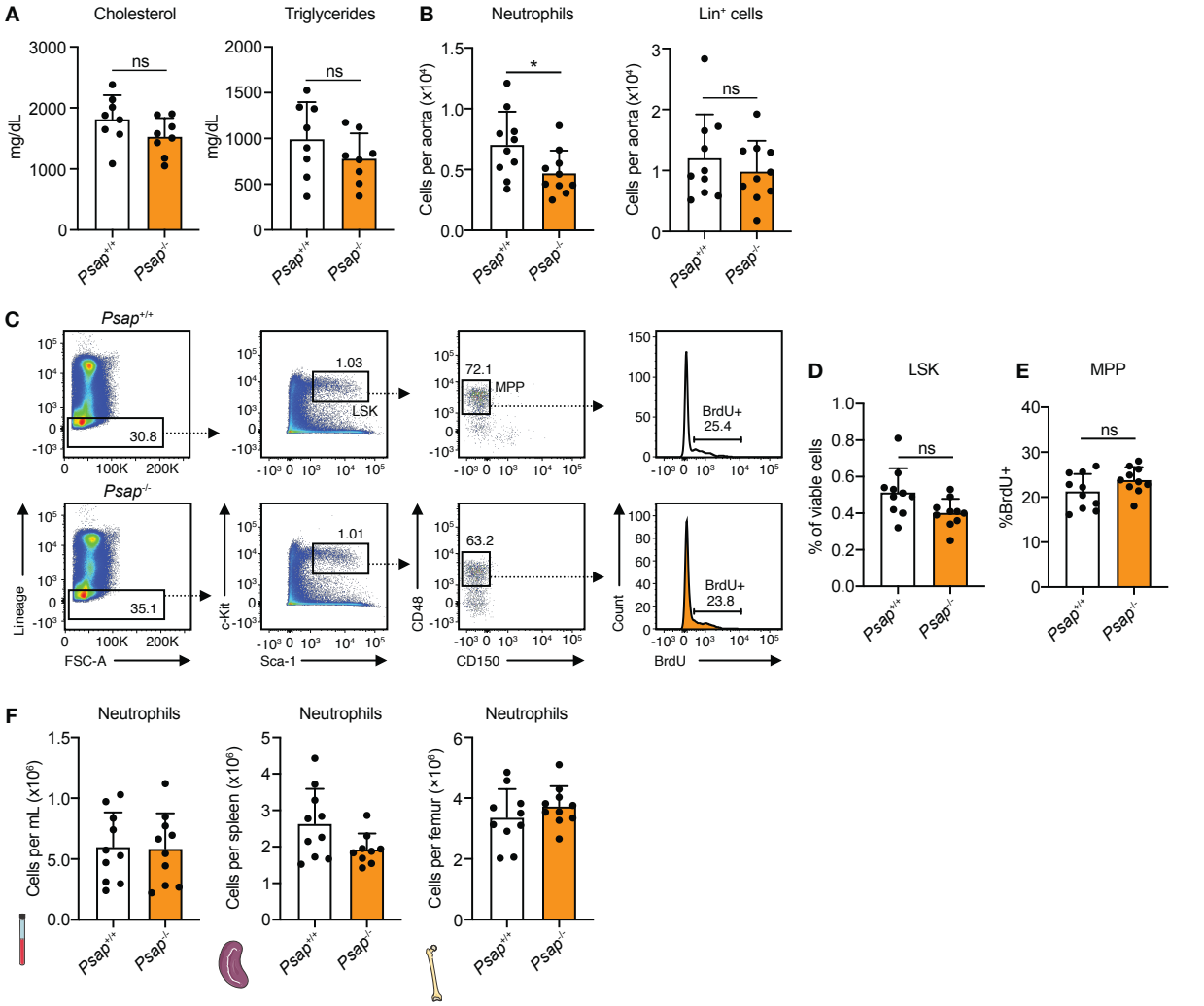


**Fig. S5. *Psap* mediates atherosclerotic plaque inflammation in *Ldlr*$^{-/-}$ mice.** Related to Figure 4. *Ldlr*$^{-/-}$ mice were lethally irradiated and transplanted with *Psap*$^{+/+}$ or *Psap*$^{-/-}$ bone marrow cells. Mice were left to reconstitute for 6 weeks after which they were fed a Western diet for 11 weeks ($n$ = 10 mice/group for all panels). (**A**) Blood cholesterol and triglyceride in *Ldlr*$^{-/-}$ mice transplanted with *Psap*$^{+/+}$ or *Psap*$^{-/-}$ bone marrow after 11 weeks of Western diet. (**B**) Flow cytometry analysis of neutrophils (CD11b$^{+}$Lin$^{+}$) and lineage positive (Lin$^{+}$) cells in the aorta of *Psap*$^{+/+}$ and *Psap*$^{-/-}$ transplanted mice. (**C**) Representative flow cytometry plots and (**D**) quantification of lineage negative, Sca1 positive, c-kit negative (LSK) cells in the bone marrow. (**E**) *Ldlr*$^{-/-}$ mice were injected with 1 mg of BrdU, 24 hours before euthanasia. Graph shows quantification of BrdU-positive multipotent progenitors (MPPs). (**F**) Neutrophils in the blood, spleen and bone marrow as assessed by flow cytometry. Experiments were performed once. Data are presented as mean ± SD. non-parametric Mann-Whitney U tests were used.

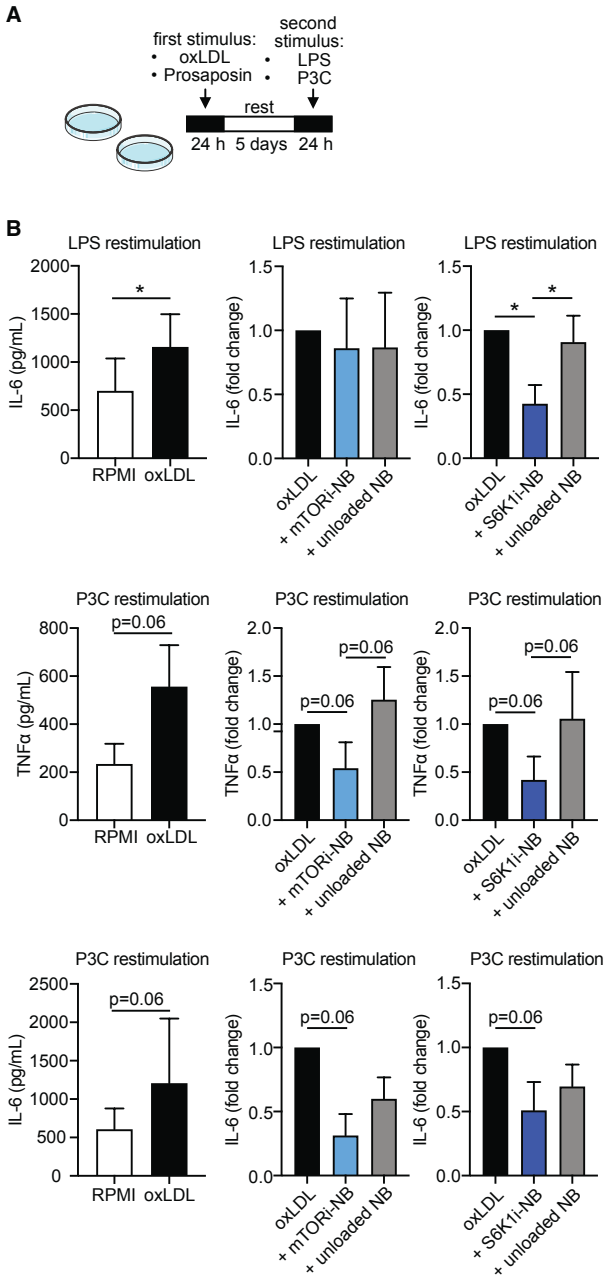


**Fig. S6. Nanobiologics inhibit oxLDL priming in human monocytes.** Related to Fig. 5.
Human primary monocytes were primed with oxidized LDL (oxLDL), in combination with mTORi-NB, S6K1i-NB, unloaded NB or RPMI for 24 hours. After a 5-day rest, cells were restimulated with LPS or Pam3Cys (P3C). This in vitro assay is schematically shown in **A**. (**B**) IL-6 and TNFα concentration upon LPS- or P3C-stimulation as measured by ELISA ($n$ = 5-6). Experiments were performed once. Bar graphs are presented as mean ± SD, Wilcoxon signed-rank tests were used. *$P$ < 0.05.

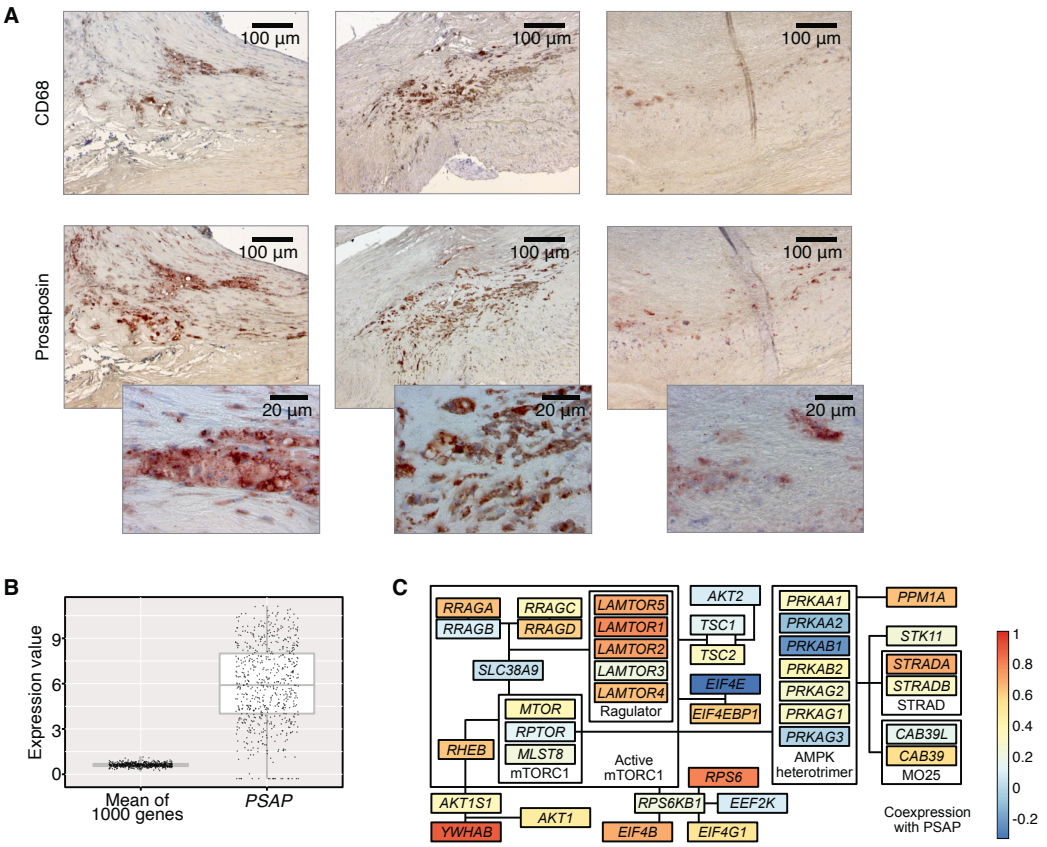


**Fig. S7. *PSAP* mediates atherosclerotic plaque inflammation in humans.** Related to Fig. 5.
(**A**) Additional images of CD68 (top) and prosaposin (middle and bottom) staining on human carotid endarterectomy samples (*n* = 4 in total). (**B**,**C**) Transcriptomic analyses were performed on human atherosclerotic plaques (*n* = 620). (**B**) Gene expression of *PSAP* as compared to the average expression of 1000 random genes was assessed showing that *PSAP* expression in the plaque is markedly higher than what can be assumed from a randomly selected gene. (**C**) Schematic representation of the genes encoding for mTOR signaling proteins. Color depicts their co-expression with *PSAP*.

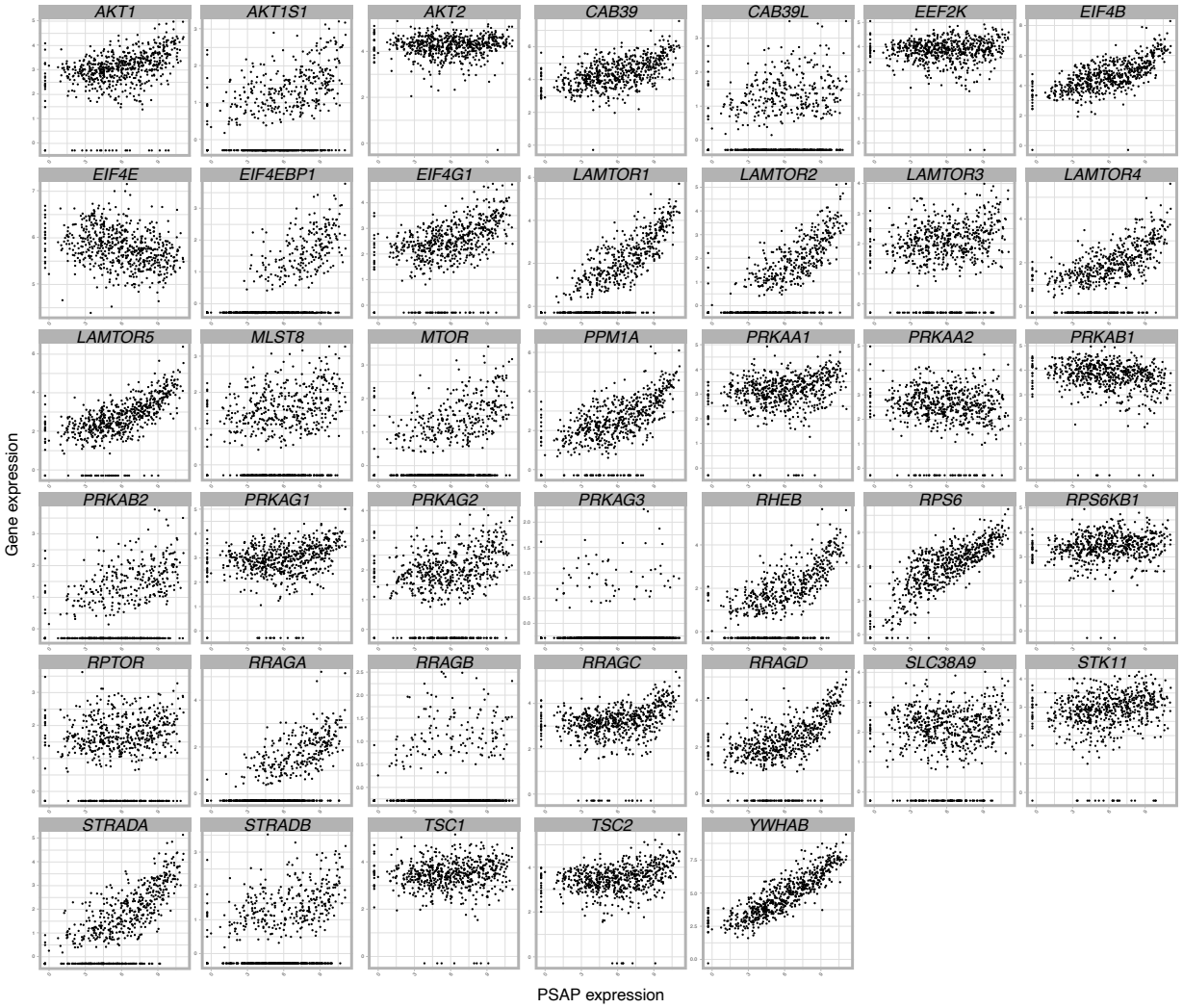


**Fig. S8. Correlation between *PSAP* expression and genes involved in mTOR signaling.** Related to Fig. 5. Transcriptomic analyses were performed on human atherosclerotic plaques (*n* = 620). Expression of *PSAP* is plotted against 40 genes involved in the mTOR signaling pathway. Each dot represents one sample.

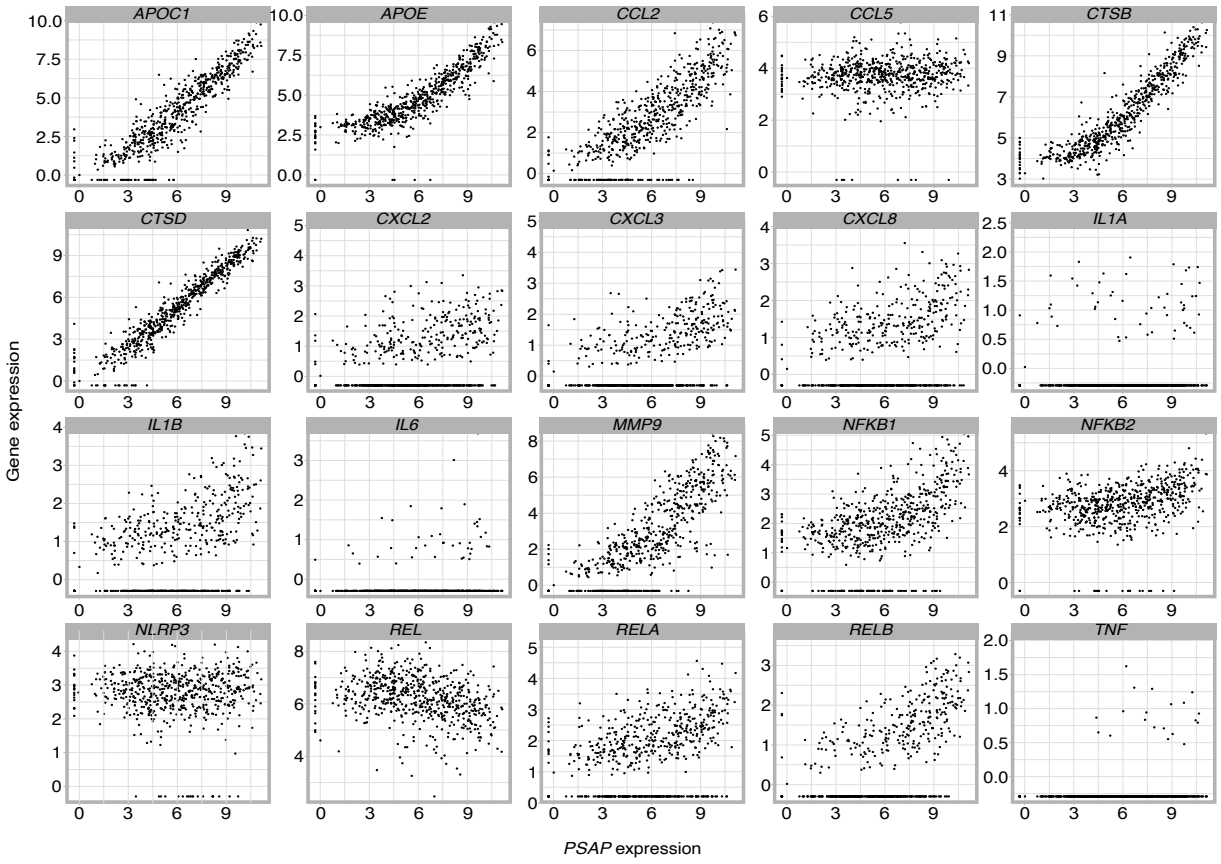


**Fig. S9. Correlation between *PSAP* expression and genes involved in macrophage inflammation.** Related to Fig. 5. Transcriptomic analyses were performed on human atherosclerotic plaques (*n* = 620). Expression of PSAP is plotted against 20 genes that define macrophage subsets in human atherosclerotic plaque. Each dot represents one sample.

**Table S1. Expression of genes coding for chemokines after mTORi-NB treatment.** Gene expression in plaque monocytes and macrophages as compared to PBS control. Log FC, log fold change.

| Gene | Chemokine | Log FC | Adjusted *P* value |
|---|---|---|---|
| *Ccl2* | CCL2 | 0.31296 | 0.65576952 |
| *Ccl3* | CCL3 | -0.39280 | 0.5613907 |
| *Ccl5* | CCL5 | 0.18974 | 0.91805817 |
| *Ccl19* | CCL19 | -0.43587 | 0.5127425 |
| *Cxcl1* | CXCL1 | 0.83790 | 0.63716585 |
| *Pf4* | CXCL4 | -1.24206 | 0.17567479 |
| *Cxcl5* | CXCL5 | 1.17180 | 0.48393745 |
| *Ccl17* | CCL17 | 1.08535 | 0.36512255 |
| *Mif* | MIF | -0.53858 | 0.17672978 |
| *Cxcl12* | CXCL12 | -0.49165 | 0.0983902 |
| *Cx3cl1* | CX3CL1 | 0.79874 | 0.0523904 |

**Table S2. Expression of genes coding for chemokines after S6K1i-NB treatment.** Gene expression in plaque monocytes and macrophages as compared to PBS control. Log FC, log fold change.

| Gene | Chemokine | Log FC | Adjusted *P* value |
|---|---|---|---|
| *Ccl2* | CCL2 | -0.00716 | 0.99102237 |
| *Ccl3* | CCL3 | 0.24487 | 0.64175807 |
| *Ccl5* | CCL5 | 0.06486 | 0.95931883 |
| *Ccl19* | CCL19 | 0.19736 | 0.7281466 |
| *Cxcl1* | CXCL1 | 1.36319 | 0.24059588 |
| *Pf4* | CXCL4 | -0.53844 | 0.45338915 |
| *Cxcl5* | CXCL5 | 0.52422 | 0.73728945 |
| *Ccl17* | CCL17 | 0.77033 | 0.43047021 |
| *Mif* | MIF | -0.31895 | 0.33069264 |
| *Cxcl12* | CXCL12 | 0.27087 | 0.28619421 |
| *Cx3cl1* | CX3CL1 | 1.04888 | 0.00247937 |

**Table S3. Expression of autophagy-related genes after mTORi-NB treatment.** Gene expression in monocytes and macrophages as compared to PBS control. Log FC, log fold change.

| Gene | Log FC | Adjusted *P* value |
|---|---|---|
| *Akt1* | -0.06322 | 0.9104776 |
| *Ambra1* | 0.47820123 | 0.17869625 |
| *App* | -0.239403 | 0.23855464 |
| *Arsa* | 0.21776034 | 0.79553701 |
| *Atg10* | 0.08458822 | 0.9259492 |
| *Atg12* | -0.4014704 | 0.38758432 |
| *Atg16l1* | 0.27097739 | 0.67061 |
| *Atg16l2* | 0.43691291 | 0.58220107 |
| *Atg3* | -0.2365799 | 0.39150025 |
| *Atg4a* | 0.04417891 | 0.97013377 |
| *Atg4b* | -0.1048479 | 0.91974653 |
| *Atg4c* | 0.13199719 | 0.82116451 |
| *Atg4d* | 0.51338288 | 0.71720056 |
| *Atg5* | -0.1456187 | 0.80253625 |
| *Atg7* | 0.1333619 | 0.75482858 |
| *Atg9a* | 0.58674968 | 0.48431597 |
| *Atg9b* | 0.44118666 | 0.81182536 |
| *Bad* | 0.41721449 | 0.67110694 |
| *Bak1* | -0.0731939 | 0.91974653 |
| *Bax* | -0.5025847 | 0.08191031 |
| *Bcl2* | 0.00557685 | 0.99301165 |
| *Becn1* | 0.17303877 | 0.8389349 |
| *Bid* | -0.3569908 | 0.47237531 |
| *Bnip3* | 0.11370475 | 0.91221636 |
| *Cln3* | -0.0844936 | 0.84365585 |
| *Cxcr4* | -0.5255795 | 0.40118318 |
| *Dram1* | 0.04323607 | 0.94370751 |
| *Dram2* | -0.195949 | 0.67061 |
| *Eif2ak3* | 0.02590746 | 0.96993217 |
| *Eif4g1* | 0.42907678 | 0.21925935 |
| *Eva1a* | -0.4900791 | 0.7507438 |
| *Gaa* | 0.10936266 | 0.85832283 |
| *Gabarap* | -0.3068282 | 0.30774929 |
| *Gabarapl1* | 0.13655259 | 0.76131999 |
| *Gabarapl2* | -0.2891248 | 0.44397101 |

| | | |
|---|---|---|
| *Hgs* | -0.0407813 | 0.96161318 |
| *Htt* | 0.10947356 | 0.79690999 |
| *Map1lc3a* | 0.27861007 | 0.75731551 |
| *Map1lc3b* | -0.0302392 | 0.94218139 |
| *Pik3c3* | 0.0621041 | 0.93584142 |
| *Pik3r4* | -0.1843173 | 0.70671046 |
| *Pten* | -0.097594 | 0.76453618 |
| *Rab24* | 0.00083353 | 0.99887287 |
| *Rgs19* | -0.0735851 | 0.8801925 |
| *Snca* | 0.56471989 | 0.8314463 |
| *Sqstm1* | -0.2376393 | 0.56678557 |
| *Ulk1* | 0.1587401 | 0.78201071 |
| *Uvrag* | 0.16747522 | 0.73636682 |
| *Vps11* | -0.2863072 | 0.45699772 |
| *Vps18* | 0.03380649 | 0.95995687 |
| *Wipi1* | -0.1570408 | 0.80540665 |
| *Wipi2* | 0.28947189 | 0.65660035 |

**Table S4. Expression of autophagy-related genes after S6K1i-NB treatment.** Gene expression in plaque monocytes and macrophages as compared to PBS control. Log FC, log fold change.

| Gene | Log FC | Adjusted *P* value |
|---|---|---|
| *Akt1* | -0.0963084 | 0.77965886 |
| *Ambra1* | 0.64609418 | 0.02107062 |
| *App* | -0.3048642 | 0.06212166 |
| *Arsa* | 0.53462818 | 0.26375584 |
| *Atg10* | -0.0908332 | 0.8721451 |
| *Atg12* | -0.5251236 | 0.12628148 |
| *Atg16l1* | 0.73261294 | 0.05882449 |
| *Atg16l2* | 0.25736148 | 0.691515 |
| *Atg3* | -0.4113048 | 0.04364753 |
| *Atg4a* | -0.518344 | 0.3527245 |
| *Atg4b* | 0.26418674 | 0.62259324 |
| *Atg4c* | 0.11796574 | 0.77911201 |
| *Atg4d* | 0.55149709 | 0.57776291 |
| *Atg5* | -0.0468501 | 0.91691084 |
| *Atg7* | 0.56047154 | 0.02530181 |
| *Atg9a* | 1.00205938 | 0.07792097 |
| *Atg9b* | -0.0311676 | 0.98354763 |
| *Bad* | 0.53327754 | 0.42217156 |
| *Bak1* | 0.29589511 | 0.40124234 |
| *Bax* | -0.6978604 | 0.00407231 |
| *Bcl2* | 0.46300037 | 0.07631071 |
| *Becn1* | 0.19421811 | 0.73879352 |
| *Bid* | -0.2469348 | 0.5277853 |
| *Bnip3* | 0.06968356 | 0.91630588 |
| *Cln3* | 0.24233459 | 0.32107786 |
| *Cxcr4* | -0.433262 | 0.38963682 |
| *Dram1* | -0.3628319 | 0.18234813 |
| *Dram2* | -0.2952424 | 0.35684941 |
| *Eif2ak3* | -0.109087 | 0.77131365 |
| *Eif4g1* | 0.43493143 | 0.12162772 |
| *Eva1a* | -1.8358585 | 0.07683732 |
| *Gaa* | 0.26790526 | 0.46088664 |
| *Gabarap* | -0.1397243 | 0.61224856 |
| *Gabarapl1* | 0.0356016 | 0.92685945 |
| *Gabarapl2* | -0.8377508 | 0.00398818 |

| | | |
|---|---|---|
| *Hgs* | 0.40132319 | 0.29166243 |
| *Htt* | 0.20689677 | 0.44036163 |
| *Map1lc3a* | 0.12440222 | 0.86633139 |
| *Map1lc3b* | -0.2246937 | 0.2339822 |
| *Pik3c3* | 0.13499383 | 0.74692382 |
| *Pik3r4* | -0.2055543 | 0.55438368 |
| *Pten* | -0.1190931 | 0.61065606 |
| *Rab24* | -0.4228867 | 0.14585505 |
| *Rgs19* | 0.19202575 | 0.48512655 |
| *Snca* | -0.4988481 | 0.80875403 |
| *Sqstm1* | -0.3630585 | 0.22598883 |
| *Ulk1* | 0.4695546 | 0.15327301 |
| *Uvrag* | 0.06612864 | 0.87435194 |
| *Vps11* | -0.0552954 | 0.87989096 |
| *Vps18* | 0.05708651 | 0.88811304 |
| *Wipi1* | -0.2248268 | 0.58860276 |
| *Wipi2* | 0.17827191 | 0.73373098 |

**Table S5. Hub genes of the mTORi-NB-related turquoise module.** Related to Fig. 2. Log FC, log fold change.

| Gene | Log FC | Adjusted *P* value |
|---|---|---|
| *Psap* | -1.0278619 | 0.01572881 |
| *Ctsb* | -0.988728 | 0.01509807 |
| *Cox7c* | -0.745240103 | 0.04504972 |
| *Rsrp1* | -1.184914126 | 0.01549977 |
| *Synpo* | 0.836086035 | 0.03921505 |
| *Flna* | 0.68071212 | 0.0305352 |
| *Hspg2* | 0.98632714 | 0.03921505 |

**Table S6. Hub genes of the S6K1i-NB-related turquoise module.** Related to Fig. 2. Log FC, log fold change.

| Gene | Log FC | Adjusted *P* value |
|---|---|---|
| *Hnrnph* | -0.674369135 | 0.009427671 |
| *Psap* | -1.219198958 | 0.001464033 |
| *Rps27a* | -1.170438898 | 0.000312172 |
| *Cox7c* | -1.048638001 | 0.001262728 |
| *Lyz1* | -1.14486756 | 0.000957917 |
| *Rn45s* | 2.281255556 | 0.00294076 |
| *Arhgdia* | 0.928242972 | 0.000311025 |

**Table S7. Correlation between *PSAP* expression and genes involved in mTOR signaling.** Related to Fig. 5.

| Gene | Estimate | Statistic | *P* value |
|---|---|---|---|
| *AKT1* | 0.45165527508346365 | 21780926.937696468 | 1.7067728486676545e-32 |
| *AKT1S1* | 0.34156205070403 | 26153965.224713564 | 2.0915357805173128e-18 |
| *AKT2* | 0.08315045831289128 | 36418391.520748235 | 0.03846760917389601 |
| *CAB39* | 0.5512671378955364 | 17824221.224209685 | 1.411655127196678e-50 |
| *CAB39L* | 0.1418716983315031 | 34085911.640083745 | 3.9502370573719507e-4 |
| *EEF2K* | 0.08099246289773902 | 36504109.75297245 | 0.043806335011565674 |
| *EIF4B* | 0.680881553419964 | 12675777.213848323 | 1.2147841466774383e-85 |
| *EIF4E* | -0.338832264388465 | 53180064.305195026 | 4.0339401091675104e-18 |
| *EIF4EBP1* | 0.6051334881203897 | 15684583.537667735 | 3.3830285221059433e-63 |
| *EIF4G1* | 0.5043801091984009 | 19686631.675105203 | 2.546435669946976e-41 |
| *LAMTOR1* | 0.7775665915236178 | 8835328.577774325 | 1.2476063535563897e-126 |
| *LAMTOR2* | 0.7117106866601788 | 11451206.121713107 | 7.418033512129724e-97 |
| *LAMTOR3* | 0.20423869897231745 | 31608617.663219813 | 2.906603831769642e-7 |
| *LAMTOR4* | 0.6263585657750161 | 14841497.346380455 | 7.291390442128253e-69 |
| *LAMTOR5* | 0.6972815335140743 | 12024349.832534747 | 1.9819847030010214e-91 |
| *MLST8* | 0.21150426467196057 | 31320020.456984177 | 1.060492246341865e-7 |
| *MTOR* | 0.38067708066467343 | 24600268.123189956 | 8.175938941027011e-23 |
| *PPM1A* | 0.631498249138613 | 14637342.801367851 | 2.654202823652396e-70 |
| *PRKAA1* | 0.30219385332589715 | 27717718.447455775 | 1.472640600777012e-14 |
| *PRKAA2* | -0.1073000560849059 | 43983320.20676145 | 0.007493408594337365 |
| *PRKAB1* | -0.24542888810671235 | 49469967.31313098 | 5.873995590121989e-10 |
| *PRKAB2* | 0.37397620432482104 | 24866435.173486788 | 5.1447710586561685e-22 |
| *PRKAG1* | 0.3066746305219916 | 27539736.46587095 | 5.733161681725475e-15 |
| *PRKAG2* | 0.2800286319529117 | 28598148.303613048 | 1.2373118951299695e-12 |
| *PRKAG3* | -0.025663298778574425 | 40740607.79334247 | 0.523586617979295 |
| *RHEB* | 0.6176288482847785 | 15188252.462645208 | 1.76153330245744e-66 |
| *RPS6* | 0.7916053124362363 | 8277693.315498397 | 2.4842854885887595e-134 |
| *RPS6KB1* | 0.19834135925734458 | 31842867.250426386 | 6.416690448822902e-7 |
| *RPTOR* | 0.12087189434866864 | 34920049.68404084 | 0.002572571027604947 |
| *RRAGA* | 0.6258121557234727 | 14863201.425712124 | 1.0332312935268605e-68 |
| *RRAGB* | 0.09268856732085305 | 36039526.09907791 | 0.020985786804036514 |
| *RRAGC* | 0.36072147214944505 | 25392929.4388133 | 1.7277295046357952e-20 |
| *RRAGD* | 0.59491515714112575 | 16090468.212711202 | 1.2828370338737115e-60 |
| *SLC38A9* | 0.04559822970010717 | 37910012.23048921 | 0.25692658759876097 |
| *STK11* | 0.24463154847624402 | 30004163.99771896 | 6.699851275922678e-10 |

| | | | |
|---|---|---|---|
| *STRADA* | 0.689009565168165 | 12352922.589755328 | 1.8383480104580137e-88 |
| *STRADB* | 0.29917553704996575 | 27837609.68246479 | 2.754917587753931e-14 |
| *TSC1* | 0.139868851242274 | 34165467.189969845 | 4.77873395253614e-4 |
| *TSC2* | 0.31993049962144865 | 27013197.04052152 | 3.195377127437807e-16 |
| *YWHAB* | 0.8807236194960035 | 4737804.54356676 | 9.61550714115254e-203 |

**Table S8. Correlation between *PSAP* expression and genes involved in macrophage inflammation.** Related to Fig. 5.

| Gene | Estimate | Statistic | *P* value |
|---|---|---|---|
| *APOC1* | 0.9243210590782618 | 3006060.6185087753 | 9.668847319715513e-261 |
| *APOE* | 0.9096722167363649 | 3587930.654405001 | 5.156031558272213e-238 |
| *CCL2* | 0.819791720688361 | 7158094.510441854 | 9.404175239057081e-152 |
| *CCL5* | 0.0997016473963565 | 35760957.93239043 | 0.013001347961345047 |
| *CTSB* | 0.9384039558518568 | 2446670.6366985515 | 2.1178347494301235e-287 |
| *CTSD* | 0.9664343657524052 | 1333268.278044592 | 0 |
| *CXCL2* | 0.3317131964009651 | 26545173.831722096 | 2.169971536107985e-17 |
| *CXCL3* | 0.48329063154314544 | 20524331.667629465 | 1.3238017390754714e-37 |
| *CXCL8* | 0.3337046358241323 | 26466071.408363402 | 1.3613214848982482e-17 |
| *IL1A* | 0.09889415971657174 | 35793032.33624132 | 0.013758140158404058 |
| *IL1B* | 0.370062481056971 | 25021893.075565413 | 1.4770067797853089e-21 |
| *IL6* | 0.1324453697499877 | 34460337.0057257 | 9.471168252244016e-4 |
| *MMP9* | 0.7988011370403015 | 7991866.311360664 | 1.6349925584291264e-138 |
| *NFKB1* | 0.5498090778999125 | 17882137.160649657 | 2.884102887438912e-50 |
| *NFKB2* | 0.38949215580494645 | 24250122.496075887 | 6.808780039263293e-24 |
| *NLRP3* | 0.02850960343379891 | 38588793.484797284 | 0.47857590568322717 |
| *REL* | -0.3503838349268979 | 53638906.89541335 | 2.393865226801823e-19 |
| *RELA* | 0.3782530901288295 | 24696552.008782033 | 1.598289081463227e-22 |
| *RELB* | 0.5603963310277618 | 17461598.44409014 | 1.4852267467657065e-52 |
| *TNF* | 0.1541101644040152 | 33599784.714370295 | 1.168669516446063e-4 |